Academic Science Journal (ASJ)
Vol. 4, No. 1, January 2026, pp. 43~58
DOI: 10.24237/04.01.425

Synthesis and characterization of (E)-5-((2-hydroxynaohthalen-1-yl) diazenyl))-2,3-dihydrophthalazine-1,4-dione complexes with Some Metal ions and their industrial and biological applications

Eman khalil Ibraham [1], Jinan M.M.Al-Zinkee [2], Amer J.Jarad [3]
[1,2] Department of Chemistry, College of Science, Diyala University, Diyala, Iraq.
[3]Department of Chemistry, College of *Education for Pure Science /Ibn-Al-Haitham*, University of Baghdad, Iraq.

Article Info

Article history:

Received 23, 12, 2024
Revised 28, 07, 2024
Accepted 10, 12, 2024
Published 30, 01, 2026

Keywords:

Azo dye complexes,
Azo dye,
Bioactivity,
Industrial applications,
Mass spectra.

ABSTRACT

When 2-naphthol is reacted with the diazonium salt of 5-amino-2,3-dihydrophthalazine-1,4-dione,(E)-5-((2-hydroxynaohthalen-yl)diazenyl))-2,3-dihydrophthalazine-1,4-dione is produced. utilised microelemental analysis (C.H.N.O.) and spectroscopic studies (FTIR, UV-Vis, ^{1}H and ^{13}C-NMR, Mass) to determine the azo ligand. . Metal chelates of transition metals were prepared and analyzed using mass spectra, atomic absorption of flame, elemental analysis, infrared and UV-Vis spectral process as well conductivity and magnetic measurements. Nature of compounds produced have been studied followed the mole ratio and continuous contrast methods, Beer's law followed during a concentration scope (1×10^{-4} - 3×10^{-4} mol/L). Height molar absorptivity of compound solutions have been noticed. Analytical data showed that all the complexes outo 1:2 metal-ligand ratio, except of palladium complex has been appeared 1:1 ratio. At the radix for physicochemical datum an octahedral structure have been described at Ni (II) and Pt (IV) complexes and square planar for Pd(II) complex Biological activity has been explored in connection to the effects of these complexes on blood lymphocyte division in the presence of PHA. The findings show that at different concentrations, Lpd causes a halt in cell division, which is more apparent. Furthermore, by generating a sustained mitotic block during the metaphase/anaphase, ligand (L) inhibited the proliferation of lymphocyte cell lines. Apart from that, using the chemicals produced to dye cotton fabric was a workable method. Dye stability under light and detergent conditions has been investigated.

Corresponding Author:

Eman khalil Ibraham
Department of Chemistry, College of Science, University of Diyala,
Al-Muqdadiya City, Diyala Governorate, Iraq.
Email: emankhilil327@gmail.com

1. INTRODUCTION

Organic chemicals, known as azo dyes, make up the majority of dye types now in use [1]. The dyes in question are highly versatile and are used extensively as organic reagents because of their great stability, fast interaction with metal ions, and high sensitivity and selectivity under complexation [2]. The synthesis of azo dyes derivatives from heterocyclic as possible scaffolds is currently receiving a lot of attention in the pharmaceutical industry. This synthetic method that can produce a variety of azo dye derivatives is required by pharmaceuticals and medical drugs [3]. Azole compounds, which are thought to be a very significant class of chemical compounds since they include a heterocyclic component, have drawn the interest of many scientists and researchers in recent years [4]. Azole dyes are among the substances with an ever-growing range of applications in analytical chemistry because they react with metal ions to exhibit distinct colour changes [5]. The extraction and measurement of trace amounts of metal ions in various materials has drawn a lot of attention to azo dyes [6][7][8]. The intriguing features of azo dye complexes and their uses as corrosion inhibitors, colourants, catalysts, antimicrobials, and anticancer agents have led to a great deal of research into these compounds [9].

In powder coating materials, electric materials, electrostatic separation processes, and electrophotographic toners, metal chalets containing azo dyes and ligand are often used as charge regulating agents [10]. We want to design and create azo compounds and their Ni(II), Pd(II), and Pt(IV) complexes of (E)-5-((2-hydroxynaohthalen-1-yl)diazenyl))-2,3-dihydrophthalazine-1,4-dione using various physico-chemical techniques. Undoubtedly, applied sciences hold significant value in the fields of chemistry, biology, and industry.

2. EXPERIMENTAL

2.1. Instrumentation

^{1}H and ^{13}C-NMR spectra were acquired using a Brucker-400 MHz Ultra Shield spectrometer in the Agilent Technologies facility at the University of Tehran, Iran. Tetramethylsaline was used as the reference and dimethylsulfoxide as the solvent. Using a Philips PW-Digital Conductance meter, the conductivity of substances dissolved in ethyl alcohol (10-3 M/L) was determined at room temperature. Micro elemental analysis (C.H.N.) was carried out with a single V utilizing the Euro vector EA 3000.3.O. Sherwood By utilizing the Auto Magnetic Susceptibility at 25oC , researchers were able to improve the magnetic properties. A Shimadzu A.A-160A Atomic Emission and Absorption of Light The atom absorption was measured using a spectrophotometer. The UV-visible spectrum was recorded using a UV-Vis-160A spectrophotometer. The spectral areas of the models were generated as KBr disks and used to generate the Shimadzu FTIR-8400S Fourier Transform Infrared Spectrophotometer's infrared spectrum at 4000-400 cm-1. Mass spectrometry measurements were carried out using a TShimadzu (E170 EV) Spectrometer. Otherwise, melting points were determined using the Stuart Melting Point Apparatus.

2.2. Materials and reagents

Following chemicals have been utilized like collected of purveyors: $NiCl_2.6H_2O$, $PdCl_2$ and $H_2PtCl_6.6H_2O$ (Merck), 3,5-dimethylphenol and 5-amino-2,3-dihydrophthalazine-1,4-dione (B.D.H) .

2.3. Preparation of the ligand

5-amino-2,3-dihydrophthalazine-1,4-dione [11] (0.442 g, 1 mmole) was melted in a combination (10 ml ethanol, 2 ml concentrated HCl), and it was diazotized at 5 oC using a 0.01 mole $NaNO_2$ solution. For the purpose of stirring a cooled ethanolic solution at 0.360 gm, 1 mmole, a diazotized solution was added collyrium-wise. After adding 25 ml of a 1M NaOH solution to a dusky-colored mixture, azo ligand precipitation was observed. After filtering and washing several ounces of the deposit in a 1:1 C2H5OH: H2O combination, the mixture was allowed to dry. The response manifests at scheme 1.

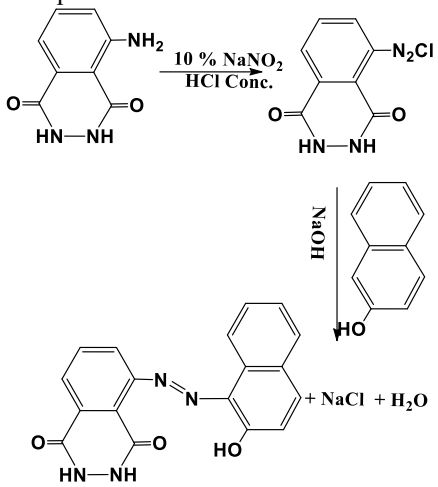

Scheme 1: Synthesis of azo ligand (L).

2.4. Buffer solution

A liter of doubly deionized water contained 0.01M (0.771 gram) of ammonium acetate dissolved in it. In order to maintain the pH range of 5 to 9, CH_3COOH or NH3 solutions had to be used.

2.5. Standard solution

pH (5–9) was used to generate mineral salt buffer solutions in the focus (10^{-5}–10^{-3} M/L) range. At the same time, a sizable volume of ethanolic ligand solutions ranging in concentration from (10^{-5}-10^{-3}) M/L were created.

2.6. Preparation of metal chelates

EtOH solution of the ligand (0.310 gm, 2mmole) was added drop wise with stirring to the 0.118, 0.117 and 0.259 gm of $NiCl_2.6H_2O$, $PdCl_2$ and $H_2PtCl_6.6H_2O$ dissolved in the buffer solution (pH=7). The mixture was cooled until dark color precipitate was contained, filtered, and washed number ounces with 1:1 H_2O: C_2H_5OH mixture. The preparation technique is shown in scheme 2, other than the physical estates and (C.H.N.) analysis is listed in Table 1.

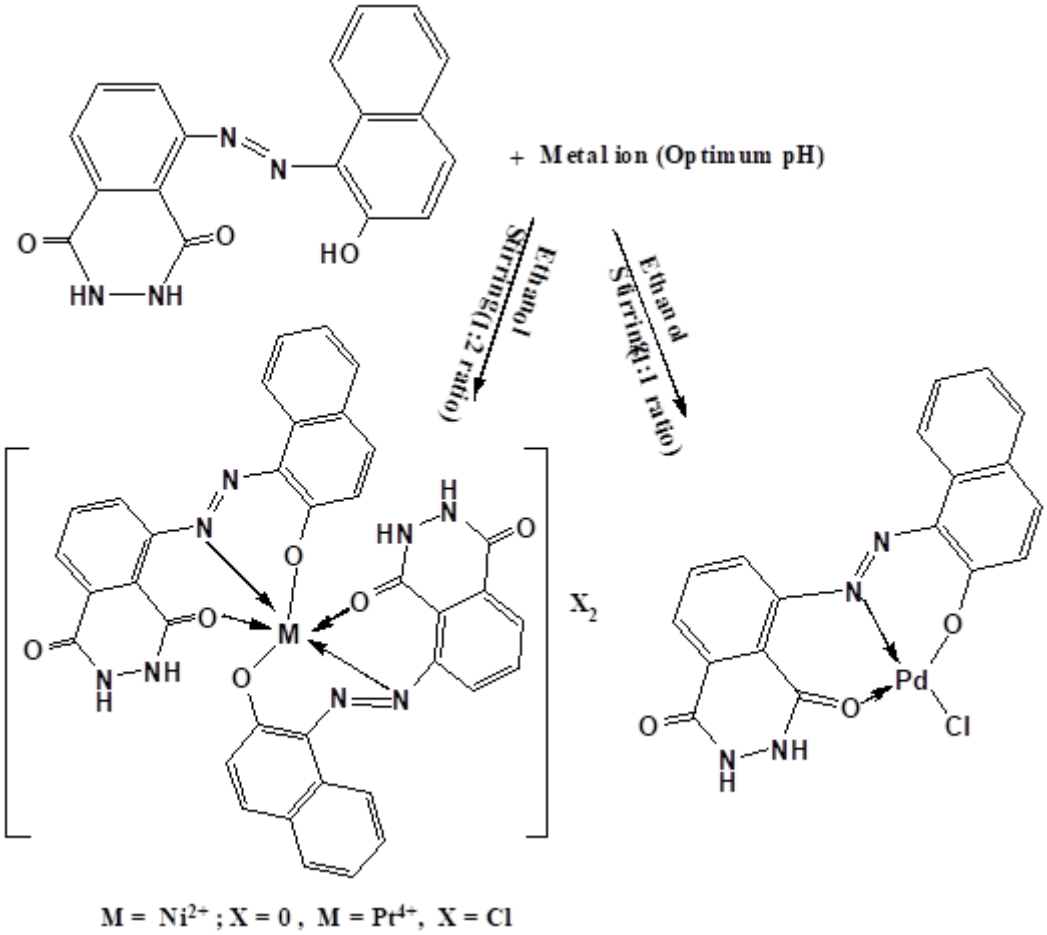

Scheme 2: Suggested structure of metal (II) complexes with azo ligand (L).

Table 1: lists the physical characteristics of metal chelates and azo ligand.

Compounds	Color	m.p°C	Yield%	Analysis Calc (Found)				
				M%	C%	H%	N%	O%
Ligand(L)	Deep red	274-276	87	-	65.06 (64.18)	3.61 (3.31)	16.86 (17.87)	14.45 (15.51)
$[Ni(L)_2]$	Greenish brown	>300	83	8.05 (7.86)	60.00 (59.75)	3.05 (2.96)	15.55 (14.92)	13.33 (12.76)
[Pd(L)Cl]	Dark brown	293-295	80	22.43 (21.83)	45.71 (44.91)	2.32 (1.97)	11.85 (10.43)	10.15 (9.84)
$[Pt(L)_2]Cl_2$	Bronze	295D	81	21.01 (20.86)	46.55 (45.74)	2.37 (1.89)	12.06 (11.74)	10.34 (9.56)

D= Dissociation

2.7. Biological part

Efficacy of Ligand and its Complexes on Human Blood Lymphatic Cell Division were studied utilizing short–repeated term culture, according to the procedure of Verma and Babu [12]. Blood samples were randomly drawn from patients of different ages by using a medical syringe containing (5ml) heparin solution for each person and utilized in the following test.

2.7.1. Transplantition of Blood and prepared compound

The compound was added at concentration of 25, 50, 100, mg/ml to the prepared culture tubes containing the complete RPMI-1640 culture medium , and the final volume of the maxture should be 5 ml , and three replicates for each concentration . Than 0.5 ml of blood was added to each tube using a 5 ml syringe , than 0.1 ml of the lymphocyte-cleaving agent (PHA)was added and mixed with the medium gently , and then incubated at 37 C on a tilted form mixed every 12 hours . Than left a group of pipes without adding any extract and this treatment was considered a control

2.7.2. Harvesting of Cell

Fifteen minutes before the original culture time ended, 0.1 ml of colchicine (10 mg/ml) was added to the control tube. The treated tubes were all put back into the incubator after no colchicine was injected. Following the incubation period, each tube was centrifuged for ten minutes at 1500 rpm. The filtrate was then disposed of, and the precipitate was thoroughly mixed with the culture medium residue.added 5–10 millilitres of 0.075 M hypotonic solution, then warmed each tube progressively and gently over the course of 30 minutes in a water bath at 37 C while shaking it. Following a 10-minute centrifugation at 1500 rpm for the tubes, the filtrate was disposed of.

2.7.3. Fixation , Washing , Dropping , Pigmentation , microscopy, and Mitotic Index

When the volume reached 5 millilitres, the precipitate was thoroughly shaken and a few drops of cold fixative were continuously shaken on the tube wall.The tubes were put at 4C for 30 minutes after the samples were combined with a Vortex. The precipitated cells were then left in the tubes, and the filtrate was disposed of after the tubes were centrifuged for 10 minutes at 1500 rpm. Until the suspension took on a distinct colour, the fixing procedure was repeated. After adding 1 millilitre of the fixative, the precipitate was suspended and kept at -20 degrees Celsius. A Pasteur pipette was used to drop the cells onto the cold, clean, wet, and fat-free glass slides from a distance of 0.5 to 1 m. The cells were then thoroughly mixed and allowed to dry on the slides. Afterwards, the slides were analysed by light microscopy to determine the Mitotic Index (ML) and stained with prepared Giemsa stain diluted with warm Sorensen buffer solution made at a ratio of 4:1 for two to three minutes. They were then rinsed with Sorensen buffer and allowed to dry. The following formula calculates the axe of the metaphase cells by the total number of cells analysed (1000).

Mitotic Index (ML) =(The number of dividing cells \|The total number of cells is 1000 100).*

2.8. The dyeing procedure

Cotton fibers are used to create and apply the chemicals, which have 1% shade painting properties. The tissue dyeing process lasts for an hour at a pH of 10 and 15–20 °C.

3. RESULTS AND DISCUSSION

Together with the proper diazotized in alkaline solution, a linked 5-amino-2,3-dihydrophthalazine-1,4-dione was created to create the azo ligand (L). Through the use of spectrum studies (^{1}H, ^{13}CNMR, Mass, FT-IR, and UV-Vis) and microelemental analysis (C.H.N.), the produced ligand was confirmed. Aqueous-ethanol solutions were created continually to examine the interaction between metal salts and the synthesised ligand.

3.1. NMR spectra

^{1}HNMR spectra of the ligand. Multiplet signals were ascribed to aromatic protons (13) at (δ=7.25-8.35) ppm in Figure 1. As opposed to this, the signals at (δ=10.55) ppm and (δ=10.15) ppm are caused by δ(OH) of naphthalene and δ(NH) of phthalazine. A reference to water and DMSO-d6 was found in signals measured at (δ=3.35) ppm and (δ=2.49) ppm (14). The carbon of the (C-OH) of naphthalene sequences and the (C=O) of phthalazine sequences were identified by signals at (δ=189.75) ppm and (δ=196.20) ppm in the 13CNMR spectra. The signals with different strengths at (δ=181.97, 178.10, 172.74, 169.75, 165.30, 157.33, 155.15, 148.96, 145.00, 137.27, 132.21, 127.48, and 118.20) ppm were associated with aromatic ring carbon atoms. Referring to Figure 2, the signal at (δ=40.79) ppm is caused by DMSO-d6 (15, 16).

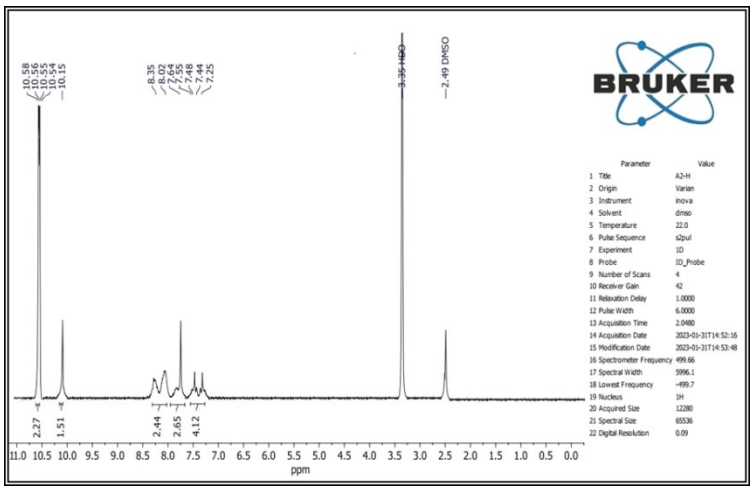

Figure 1: The azo ligand (L) ^{1}HNMR spectrum.

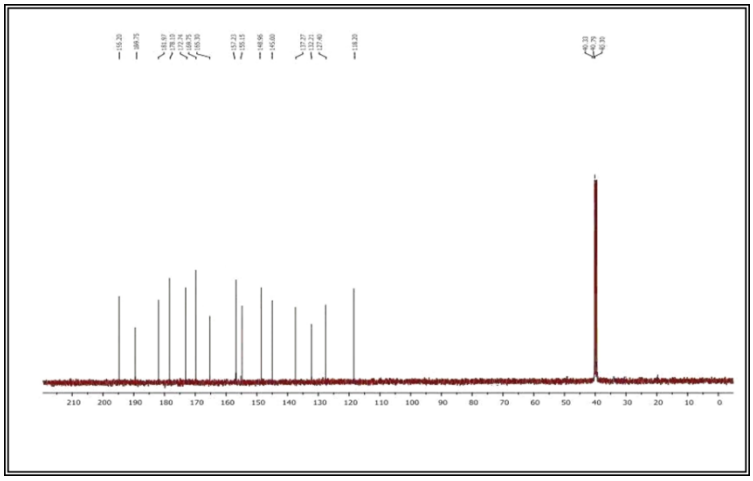

Figure 2: The azo ligand (L) in the ^{13}CNMR spectrum.

3.2. Mass spectra

The formula $C_{18}H_{12}N_4O_3$ exhibited a peak at m/z = 332 in the mass spectrum of the azo ligand (L). Figure 3 shows Scheme 3, which summarises the basic fragmentation pattern. With respect to the formulations $C_{36}H_{22}N_8O_6Ni$, $C_{18}H_{12}N_4O_3ClPd$, and $[C_{36}H_{22}N_8O_6Pt]^{2+}$, the mass spectra for metal complexes' show peaks centred at m/z = 720, 472.5, and 857 and so on. Please refer to Figures 4 and Figure 5 and 6 for a summary of the general fragmentation pattern.

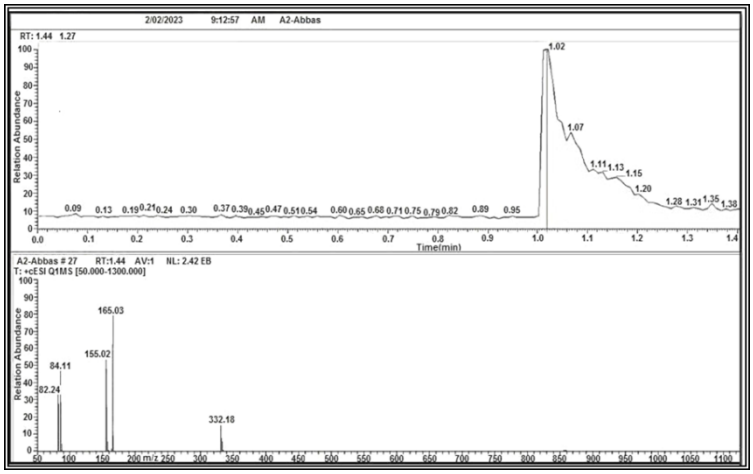

Figure 3: The azo dye ligand (L) mass spectrum.

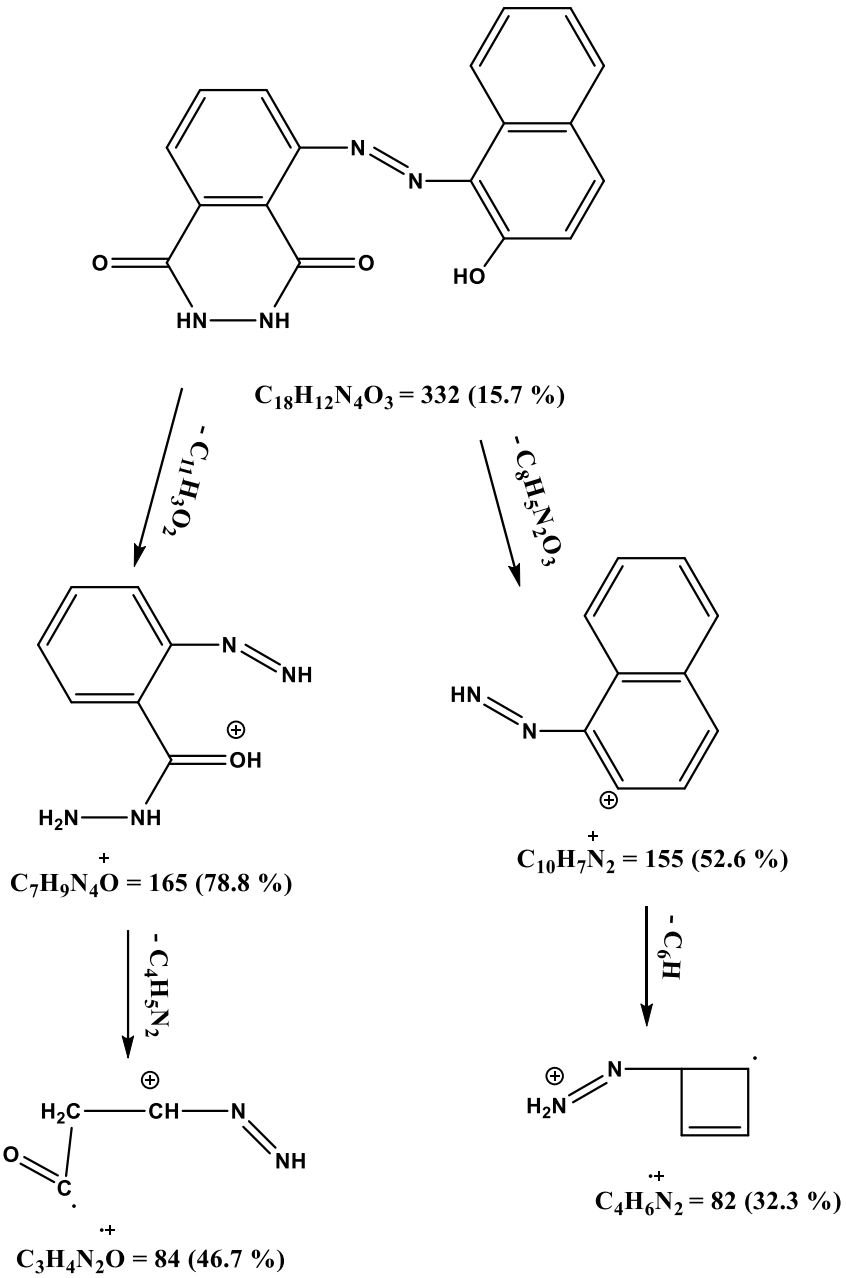

Scheme 3: The azo dye ligand fragmentation pattern (L)

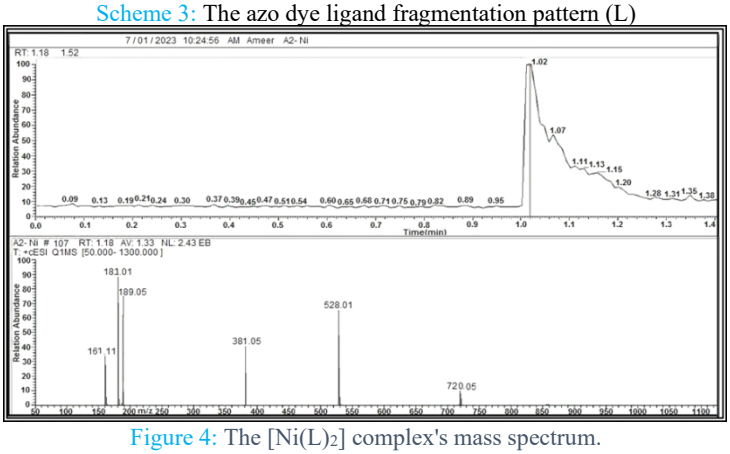

Figure 4: The $[Ni(L)_2]$ complex's mass spectrum.

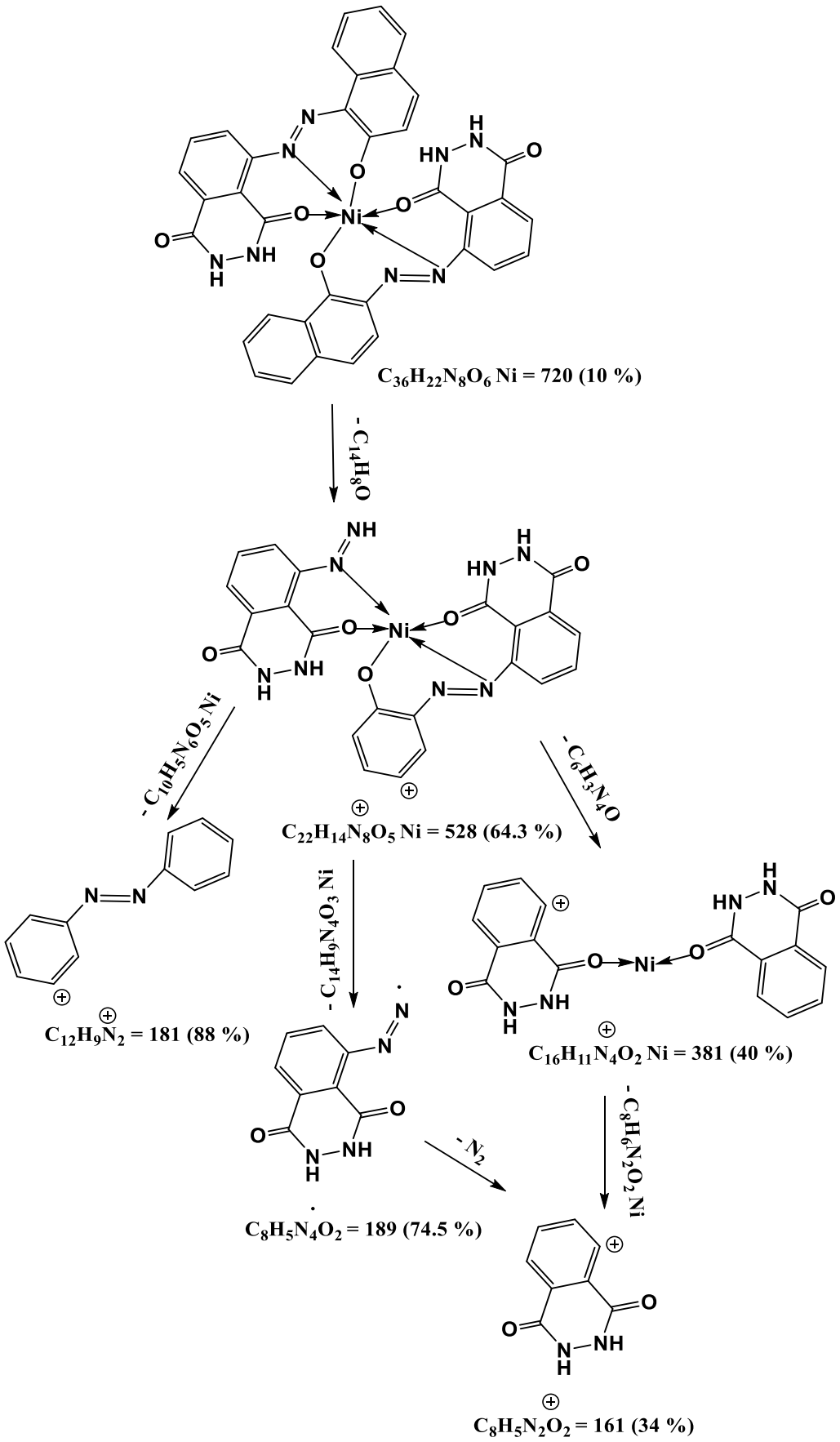

Scheme 4: Fragmentation pattern for $[Ni(L)_2]$ complex.

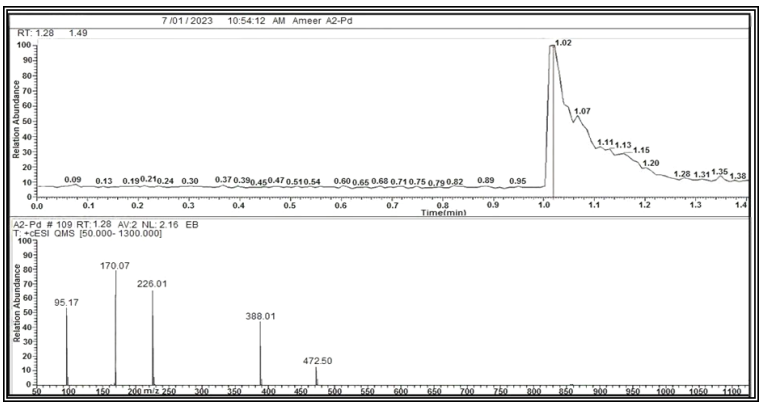

Figure 5: The [Pd(L)Cl] complex's mass spectrum.

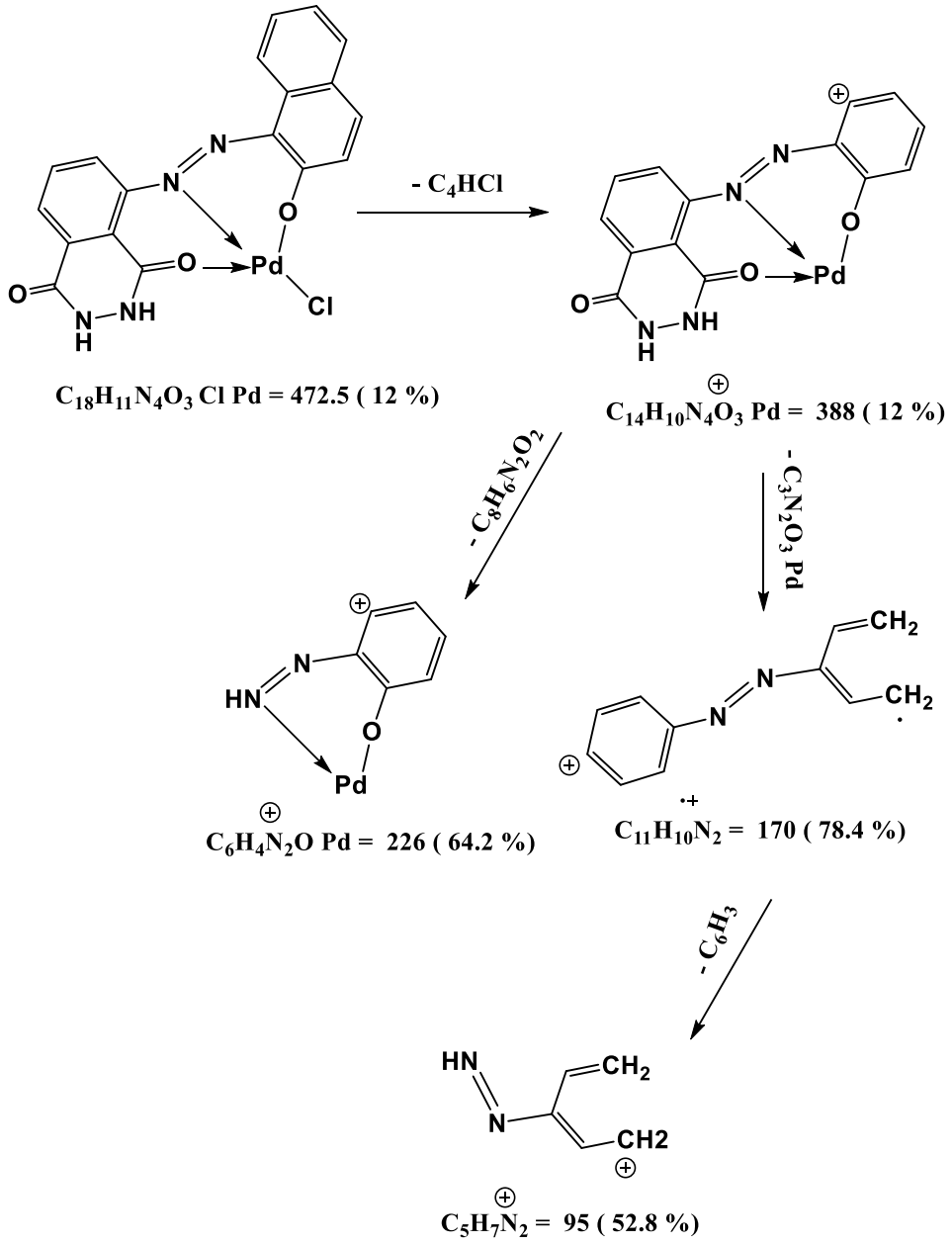

Scheme 5: Fragmentation pattern for [Pd(L)Cl] complex.

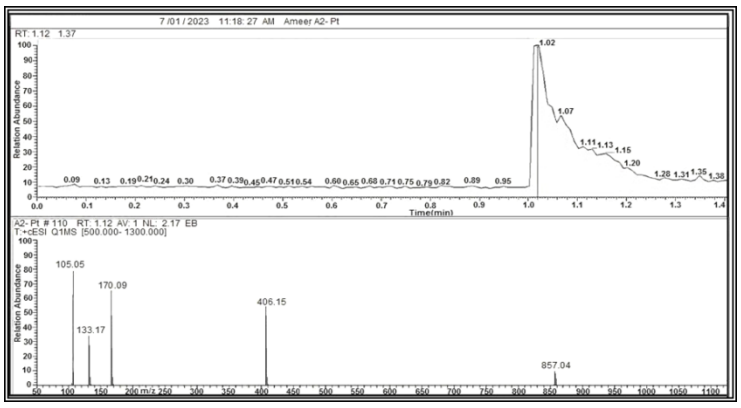

Figure 6: The $[Pt(L)_2]Cl_2$ complex's mass spectrum.

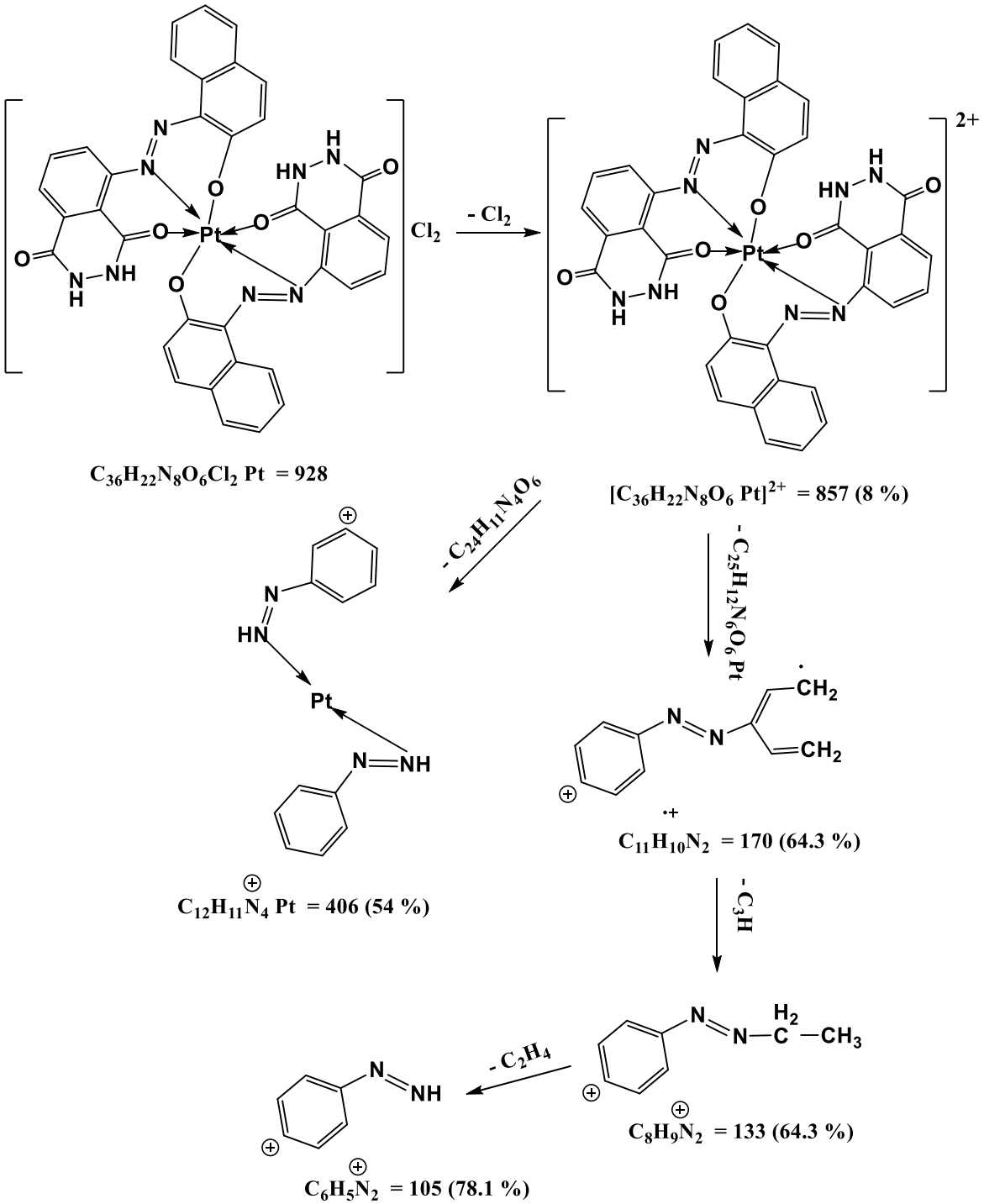

Scheme 6: Fragmentation pattern for $[Pt(L)_2]Cl_2$ complex.

3.3. Calibration curve

The only molar concentrations (10^{-5}-10^{-3} M/L) that combined with metal ions and aqueous ethyl alcohol ligand that fit Beer's law and appeared bright were (1-3 x 10^{-4} M/L). Figure 7 shows the correlation factor R > 0.998. The best and most acceptable straight lines are selected.

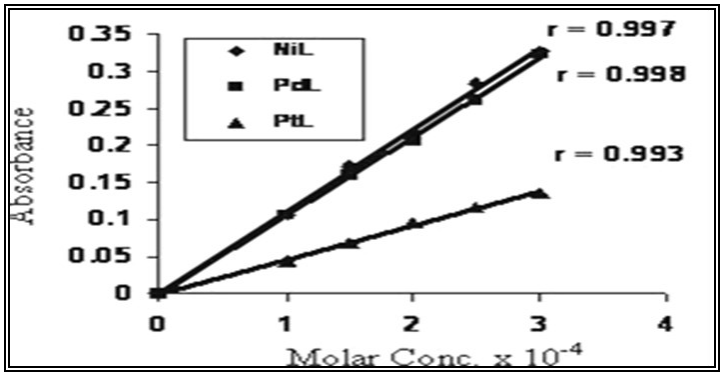

Figure 7: The connection between molar concentration and absorbance.

3.4. Typical conditions

When creating compounds, the spectrum of ligand-metal ion mixing solutions is the first test to look for interactions between synthesized ligand and poorly interacted metal ions in order to improve pH, focus, and wavelength (max). In the produced compounds, the metal to ligand ratio (M:L) was also ascertained. The best concentration was determined by selecting the solution that produced the maximum absorption at a constant (max) while varying pH. The results are shown in Table 3. The outcomes of the experiment demonstrate that every chemical produced absorbs in an NH_4OOCCH_3 buffer solution at a pH of 5–9. Figure 8 illustrates that every produced chemical has an accurate pH.

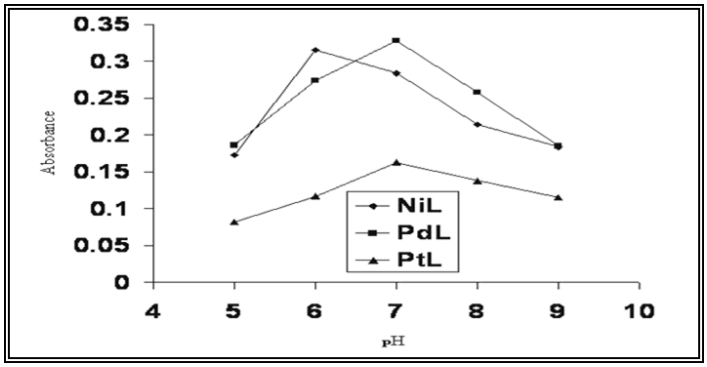

Figure 8: Effect of pH at absorption (λmax) to the compounds.

3.5. Metal to ligand ratio

The complexes have been placed in solutions using the mole ratio approach. With the exception of Pd(II), which had a ratio of 1:1, under both conditions, the results showed 1:2 (metal to ligand); see Figure 9. Results filtered and specifications into compound creation are summarized in Table 3.

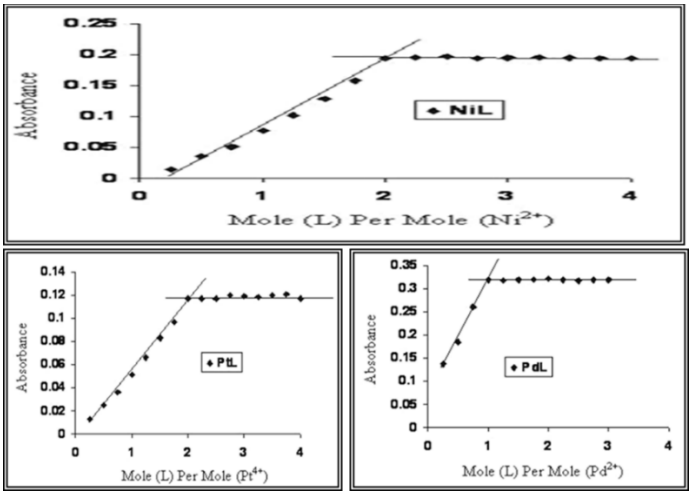

Figure 9: Mole ratio for the compounds solutions.

3.6. The Effect of time

This response occurred in five minutes. Because of the high coordination of bonds with metal-salts, the temperature was set at 25 °C and stayed there for around 90 minutes. The outcomes are displayed in Figure 10.

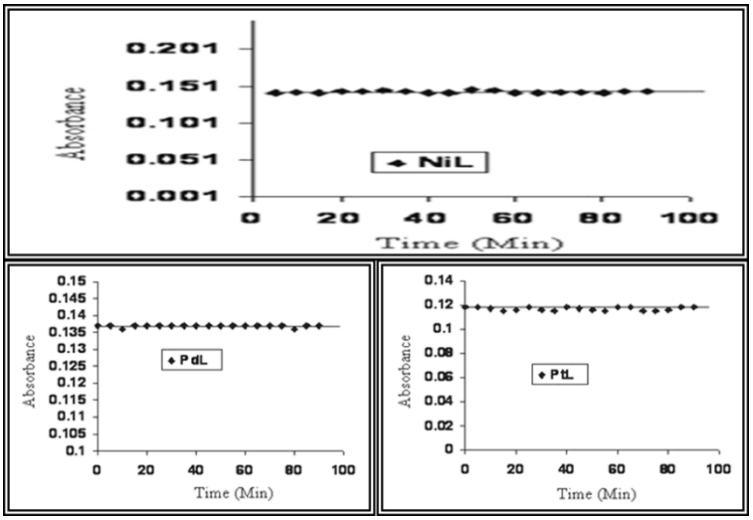

Figure 10: Effect of time on the produced compounds.

3.7. Stability constant and Gibbs free energy

The following equations can be used to calculate the stability constant (K) for the metal to ligand complex (1:2):

$$K = \frac{1-\alpha}{4\alpha^3 C^2} \quad ; \qquad \alpha = \frac{A_m - A_s}{A_m}$$

While the ratio (1:1, M:L) calculated according to the equation :

Am denotes the absorption of a solution containing excess ligand and self-same amounts of metal, c is condensation to the compound solution at mole / L, and As indicates absorption in a solution containing the same quantity of ligand and metal ion. Robust (K) values (17) are indicative of robust complicated production consistency. Researchers also looked into the thermodynamiccharacteristicsof Gibbs free energy (ΔG). Equation (18) was utilised to calculate the ΔG data.

$$\Delta G = - R\,T\,Ln\,k$$

Under the following conditions: T = absolute temperature (Kelvin), R = gas constant = 8.314 J.mol-1.K, and the negative value of (G) resulting from the spontaneous reaction between azo dye ligands and metal ions under study. Table 2 presented all of the results.

Table 2: Stability constant and Gibbs free energy of the prepared complexes.
3-8-Physical properties

Complexes	As	Am	α	K	Ln k	ΔG kJ.mol^{-1}
$[Ni(L)_2]$	0.077	0.194	0.603	7.352×10^6	15.810	- 39.170
[Pd(L)Cl]	0.319	0.321	0.006	1.104×10^6	18.519	- 45.882
$[Pt(L)_2]Cl_2$	0.051	0.177	0.712	3.236×10^6	14.989	- 37.136

3.8. Physical properties

When the metal ions dissolved in a buffer solution (pH=7) with a (Metal:Ligand) ratio of (1:2), except for Pd(II), which was rated at 1:1, the ligand melted in ethanol interacted with the metal ions to form solid complexes. Accurate estimates were used to reach the same conclusion regarding the elemental analysis result and the metal contained in compounds. The conductivity of metal chelates and ligands melted in dimethylsulfoxide (10 -3 mol/L) shows a non-electrolytic type (19), except for the platinum complex in Figure 3, which seems to have a 1:2 electrolyte nature ratio.

3.9. Electronic spectra

UV-Vis spectra of azo ligand (L) and their metal chelates melted at ethanol (10-3 mole/L) were gauged as well the data formed are recorded at Table 3. Spectrum of azo ligand (L), exhibited peaks at 273 and 350 nm which were assigned to (π-π*) .Other peak at 482 nm due to (n-π*)(20). NiII complex displayed two absorption peaks at 244 and 510 nm which were described to intra ligand and (M→L) charge transfer with electronic transition type $^3A_{2g(F)} \rightarrow {}^3T_{1g(P)}$. Peaks at 778 and 888 nm which were assigned to electronic transition type $^3A_{2g(F)} \rightarrow {}^3T_{1g(F)}$ and $^3A_{2g(F)} \rightarrow {}^3T_{2g(F)}$, magnetic moment of this

complex was found at 2.92 B.M which was very close to the octahedral environment(21). Spectrum of PdII complex showed peaks at 352 nm and 490 nm described to intra ligand and (M→L) charge transfer. Peaks at 630 and 778 nm which were assigned (22) to $^1A_{1g} \rightarrow {}^1B_{1g}$ and to $^1A_{1g} \rightarrow {}^1A_{2g}$. PtII spectrum showed peaks at 352 and 492 nm attributed to intra ligand and (M→L) charge transfer. Peak at 778 nm due to $^1T_{1g(F)} \rightarrow {}^1A_{2g(F)}$ (23).

Table 3: Conditions of the generated compounds and the datum of conductance measurement, magnetic susceptibility, and UV-visible.

Compounds	Optimum pH	Optimum Molar Conc. x 10^{-4}	M:L Ratio	(λ_{max}) Nm	ABS	ϵ_{max} (L.mol^{-1}.cm^{-1})	Λ_m(S.cm^2.mol^{-1}) In DMSO	μ_{eff} (B.M)
Ligand(L)	-	-	-	273 350 482	0.863 0.311 0.214	863 311 214	-	-
[Ni(L)$_2$]	7	2.5	1:2	244 510 778 888	1.455 0.730 0.076 0.078	1455 730 76 78	16.72	3.01
[Pd(L)Cl]	7	2.5	1:1	352 490 630 778	0.488 0.190 0.052 0.083	488 190 52 83	12.66	Dia
[Pt(L)$_2$]Cl$_2$	7	2.5	1:2	352 492 778	0.2290.156 0.021	229 156 21	72.61	Dia

Dia = Diamagnetic

Table 4: Infrared spectra (cm-1) of the azo ligand (L) and its metal chelates

Compounds	υ(OH) + υ(NH)	υ(C=O)	υ(C=C)	υ (N=N)	υ(M-N) + υ(M-O)
Ligand(L)	3483 sh. 3414 sh. -	1662 s. 1678 sho. 1654 s.	1589 sh. 1570 sho. 1531 s.	1442 sh. 1423 sh. 1396 sh. 1342 sh.	-
[Ni(L)$_2$]	- 3421 br.	1678 sh. 1639 s.	1597 sh. 1586 sho. 1512 sh.	1527 sh. 1446 sh. 1419 sh. 1357 sh.	459 w. 432 w.
[Pd(L)Cl]	- 3425 br.	1678 s. 1635 sho.	1597 sh. 1572 sho. 1519 sh.	1450 sh. 1423 sh. 1392 sh. 1357 s.	470 w. 451 w.
[Pt(L)$_2$]Cl$_2$	- 3479 br.	1678 sh. 1620 sho.	1600 sh. 1558 sho. 1508 sh.	1454 sh. 1427 sh. 1396 sh. 1357 sh.	482 w. 451 w.

br=broad, sh = sharp, s = strong, w = weak, sho =shoulder

3.10. FTIR spectra

Table 4 presents the data that was gathered from the spectra of azo ligand (L) and its metal chelates. All generated compounds' spectra indicated the deprotonation of the hydroxyl group to coordinate with the metal ion, as seen by the band at 3452 cm-1 in the ligand spectrum that was attributed to stretching vibration of υ(OH)(24). This group's band at 3379 cm-1 is caused by υ(NH), but no discernible change in this band was observed, ruling out the notion that coordination occurs through the contributing atom (25). Due to the υ(C=O) and υ(N=N) vibrations, the spectrum showed bands at 1662 cm-1 and 1527 cm-1. These bands were eliminated upon complexation, indicating a coordinated with a metal ion, (26). In complex spectra, bands attributable to υ(C=C)(27) emerged at (1597-1554) cm-1. According to the presence of the bands at a rate of 576-466 cm-1, stretching frequency bands to metal-nitrogen on different metal-oxygen more (28, 29) is guaranteed.

3.11. Antimicrobial testing outcome

Biological part

Effect of the ligand and its complexes on Lymphatic Cell division in Human Blood

Figure 11 shows the effect of Colchicine, ligand and its complex on Lymphatic Cell in metaphase in human blood. The percentage of suspended cells stopped in the metaphase of the ligand (L) was 1.23, 2.37, 3.78 at concentrations 25, 50, 100 µg /ml respectively, while the percentage of stopped cells in the control was 4.13. and The percentage of suspended cells stopped in the metaphase of the platinum complex [Pt $(L)_2$] Cl_2 was 0.95, 1.16 , 1.57 at concentrations 25, 50, 100 µg /ml respectively, while the percentage of stopped cells in the control was 4.33, and The percentage of suspended cells stopped in the metaphase of the palladium complex [Pd(L)]Cl was 0.00, 0.01, 1.04 , at concentrations 25, 50, 100 µg /ml respectively, while the percentage of stopped cells in the control was 4.33, as shown Table 5 [30]. The results showed The effect of ligand and their complexes (L pt and Lpd) on the lymphocytes proliferation cell line was lowest inhibition rate 0.00b ± 0.11at the concentration 25 Mg/ml and higher inhibition rate was 1.04 b ± 0.08 at the concentration 100 Mg/ml for Lpd. While in the L lymphocytes proliferation cell line the lowest inhibition rate was 1.23 b ± 0.01 at the concentration 25 Mg/ml and higher inhibition rate was 3.78 d ± 0.02 at the concentration 100 Mg/ml the results showed that the (L) has the ability to stop lymphocyte division in the tropic phase through its effect on microtubules and this on spindle filaments

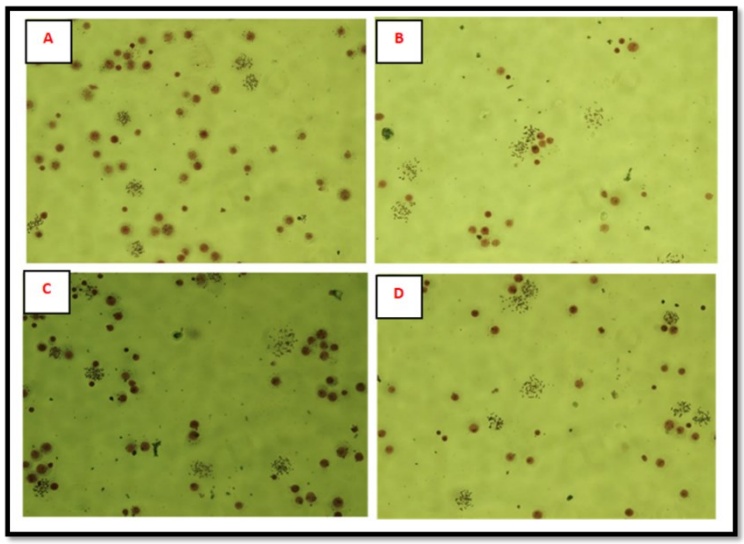

Figure 11. humans lymphocytes in metaphase treatment with (A) Colchicine , (B)L, (C) [Pt (L)2]Cl2 , (D)[Pd (L)]Cl in concentration 100mg/ml

Table 5. Study the effect of (L, Lpt, Lpd) in Mitotic Index (chromosome) in lymphocytes of humans.

Concentration (µg/ml)	L The percentage of cells in the tropical phase inhibition ±standard deviation	Lpt The percentage of cells in the tropical phase inhibition standard deviation±	Lpd The percentage of cells in the tropical phase standard deviation± inhibition
Control (cholgsen)	4.13a ± 0.11	4.33a ± 0.01	4.33a ± 0.01
25	1.23b ± 0.01	0.95d ± 0.10	0.00b ± 0.11
50	2.37c ± 0.11	1.16d ± 0.11	0.01b ± 0.10
100	3.78d ± 0.02	1.57c ± 0.01	1.04b ± 0.08

3.12. Dyeing performance

The efficacy of the finished chemicals in dying cotton textiles has already been established. The colors contributed to the brightness and stability of the detergent. Complete dyes therefore show excellent textural depth and dyeing stability. Figure 12 shows coloring.

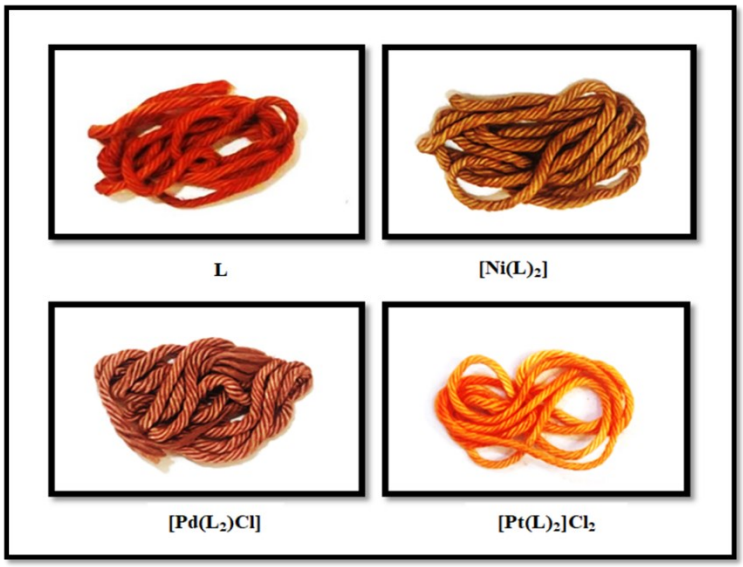

Figure 12. Textiles dying by azo ligand (L) and it complexes.

4. CONCLUSION

In this work, we synthesised and characterised its spectra of a novel azo dye ligand, which was obtained by reacting 2-naphthol with 5-amino-2,3-dihydrophthalazine-1,4-1. azo ligand was identified by means of microelemental analysis (C.H.N.O.) and spectroscopic studies (FTIR, UV-Vis, 1H and 13CNMR, Mass) as well as its metal complexes with Ni(II), Pd (II), and Pt (IV) ions.Additionally, a number of metal complexes were created and evaluated using mass spectra, elemental analysis, UV-Vis and infrared spectral processes, as well as conductivity and magnetic quantifications. Only the palladium complex emerged in a 1:1 ratio, according to analytical data, indicating that the other compounds outperform in the 1:2 metal-ligand ratio range. Octahedral structures for Pt(IV) and Ni(II) complexes and square planar structures for Pd(II) complexes have been reported at the radix for physicochemical datum. The influence of complexes on blood lymphocyte division in the presence of PHA was examined, and the findings indicated that the pd complex inhibited cell division at various doses and that this inhibition grew. By producing a persistent mitotic block at the metaphase/anaphase boundary, ligand (L) also prevented the growth of lymphocyte cell lines.

ACKNOWLEDGEMENTS

The author gratefully acknowledges the support of Chemistry Department at the University of Diyala.

Conflict of interest: no conflict

Ethical Clearance Statement (Inorganic Chemistry)

This research was conducted in the field of Inorganic Chemistry and does not involve human participants, clinical/human samples, or live animals. As such, the need for approval from an Institutional Review Board (IRB) was waived by [university of Diyala, college of sciences) All relevant institutional guidelines regarding laboratory safety and the use of chemical materials were adhered to.

REFERENCES

[1] Ali, R.R. and Mohammed, H.S. 2021. Synthesis and characterization and biological study of pyridylazo ligand and its compounds of Co, Ni and Cu divalent ions, Journal of Physics: Conference Series, 1999, 012009. DOI: 10.1088/1742-6596/1999/1/012009

[2] Mohammed,H.S.,Tripathi, V.D. and Darghouth, A.A. 2019 Synthesis, Characterization, DFT calculation and Antimicrobial Activity of Co (II) and Cu(II) complexes with azo dye, Journal of Physics: Conference Series, 1294, 052051. DOI: 10.1088/1742-6596/1294/5/052051

[3] Bouhdada, M., Amane, M.E. and El Hamzaoui, N. 2019. Synthesis, spectroscopic studies, X-ray powder diffraction data and antibacterial activity of mixed transition metal complexes with sulfonate azo dye, sulfamate and caffeine ligands, Inorganic Chemistry Communications, 10,1 32–39. https://doi.org/10.1016/j.inoche.2019.01.005

[4] Sayhood, A.A. and Mohammed, H. 2015. Synthesis of new azo reagent for determination of Pd(II),Ag(I) and applied to enhance the properties of silver nano particles, Int. J. Chem. Sci., 13(3),1123-1136.

[5] Ali1, F.J., AL-Ameri, L.A.M. and Ali, A.M. 2021. Synthesis and identification and biological studies of new azo dyes derived from imidazole and their chelate complexes, Indian Journal of Forensic Medicine and Toxicology, 15(2),1253-1260. https://doi.org/10.37506/ijfmt.v15i2.14496

[6] Mahmoud, W.H., Sayed, F.N. and Mohamed, G.G. 2016. Synthesis, characterization and in vitro antimicrobial and anti-breast cancer activity studies of metal complexes of novel pentadentate azo dye ligand, Applied Organometallic Chemistry, 30(11), 959–973.
[7] Manna, C.K., Naskar, R. and Mondal, T.K. 2019. Palladium (II) complex with 1-(2-pyridylazo)-2-naphthol (PAN): synthesis, X-ray structure, electrochemistry, DFT computation and DNA binding study," Journal of the Indian Chemical Society, 96(5),599–606. https://doi.org/10.1016/J.POLY.2018.04.044
[8] Abd El-Wahaab, B., Elgendy, K. and El-didamony, A.2020. Synthesis and characterization of new azo-dye reagent and using to spectrophotometric determination of samarium(III) in some industrial and blood samples, Chemical Papers, 74(5),1439–1448. https://doi.org/10.1007/s11696-019-01000-8
[9] Abate,P.O., Sottile,M., Le´on,I.E., Vergara,M.M. and Katz,N.E. 2020. symmetrical dirhenium(I) complex with 4,4''-Azobis(2,2'-bipyridine) as a bridging ligand: synthesis, physicochemical properties and applications in detection of biologically relevant thiols and in chemotherapy for bone cancer, Journal of the Brazilian Chemical Society, 31(11), 2299–2306. https://doi.org/10.21577/0103-5053.20200085
[10] AL-Adilee,K.J., Abass ,A.K. and Taher,A.M. 2016. Synthesis of some transition metal complexes with new heterocyclic thiazolyl azo dye and their uses as sensitizers in photo reactions, Journal of Molecular Structure, 1108, 378e397. http://dx.doi.org/10.1016/j.molstruc.2015.11.038
[11] Al-Zinkeei,J.M.M. and Jard.A.J. 2019. Synthesis, characterization and microbial evaluation of heterocyclic azo dye ligand complexes of some transition metal(II) Ions, Asian Journal of Chemistry,31(3),727-732. https://doi.org/10.14233/ajchem.2019.21800
[12] Verma, R. S., & Babu, A. (1989). Human chromosomes: manual of basic techniques.
[13] Carballo,R., Castineras,A., Covelo,B., Niclos,J. and Vazjuez-Lopez,E.M. 2001. Synthesis and characterization of a potassium complex of magneson: [K(HL)(OH2)2]∞ [H2L=4-(4-nitrophenylazo)resorcinol (magneson)], Polyhedron, 20,2415-2420. DOI: 10.1016/S0277-5387(01)00842-7
[14] Fayadh,R.H., Ali,A.A. and Al-Jabri,F.M. 2015. Synthesis and identification symmetrically azo dyes derived from sulfa compounds and spectrophotometric study of Nickel (II) complexes with prepared dyes, International Journal of Engineering and Technical Research, 3(3),24-28.
[15] Adbulrazzaq,A.G. and Al-Hamdani, A.A.S. 2023. Some metal ions complexes with azo [4-((8-hydroxyquinolin-7-yl)-N(4-methylisoxazol-3-yl)benzenesulfonamide] :Synthesis, characterization, thermal study and antioxidant activity. Journal of Medicinal and Chemical Sciences, 6(2),236-249. DOI: 10.26655/JMCHEMSCI.2023.2.7
[16] Nguyen,A.V., Vu,A.T.N., Bazan,L.V., Galeev, R.T., Utenyshev,A.N., Markova, E.B., Le, V.T. and Kovalchukova, O.V. 2022. Synthesis, characterization and sorption activity of novel azo-colorants derived from phloroglucinol and antipyrine and their metal complexes. Royal Society of Chemistry, 12,888-898. https://doi.org/10.1039/D1RA07254D
[17] Cao,H.W and Zhao,J.F. 2003. Stability constants of cobalt(II) and copper(II) with 3-[(o-carboxy-p-nitrobenzene)azo] chromotropic acid and selective determination of copper(II) by competition coordination, Croatica Chemica Acta.,76,1-6.
[18] G.Wtter, N.Ludwig and S.Horst; "Thermodynamics and statistical mechanics", Springer-Verlag, (1996)101.
[19] Geary, W.J. (1971) The Use of Conductivity Measurements in Organic Solvents for the Characterisation of Coordination Compounds. Coordination Chemistry Reviews, 7, 81-122. http://dx.doi.org/10.1016/S0010-8545(00)80009-0
[20] Ibraham, EK, Al-Zinkee, JMM, Jarad, AJ. Feasible and simple preparation of Pd (II), Ni (II), and Pt (IV) complexes: Their biological and industrial applications and investigation of Pd (II) complex in Suzuki reaction. Iranian Journal of Catalysis.2024; 14(2): 142419 (1-17). https://doi.org/10.57647/j.ijc.2024.1402.19
[21] Patel,K.D. and Patel,H.S. 2017. Synthesis, spectroscopic characterization and thermal studies of some divalent transition metal complexes of 8-hydroxyquinoline, Arabian Journal of Chemistry, 10, S1328–S1335. https://doi.org/10.1016/j.arabjc.2013.03.019
[22] Al- Hasani, T.J. and Almaliky,Z.S. 2015. New Pd and Pt complexes of guanine –azo dye: structural, spectroscopic, dyeing performance and antibacterial activity studies, Iraqi Journal of Science, 56(4A), 2718-2731.
[23] Hussein,A.O., Abbas,R.A., Sultan,J.S. and Jarad,A.J. 2020. Synthesis and characterization of metal(II) complexes with azo dye ligand and their industrial and biological applications. Egyptian Journal of Chemistry, 64(11),6717-6724. DOI: 10.21608/EJCHEM.2021.68770.3530
[24] Jarad,A.J.,Kadhim,Z.S., Mahmood,M.A. and Obaid,S.M.H. 2016. Synthesis, spectral studies and biological activity of azo dye complexes with some metal ions. Journal of Global Pharma Technology, 10(06)97-106.
[25] Jarad,A.J. and Quiasim,S.H. 2018. Synthesis and characterization of azo dyes ligands complexes with Ni(II) and Cu(II) and studies their industrial and bacterial application. Research Journal Pharmaceutical ,Biological and Chemical Science, 9(2),631-642.
[26] Jarad,A.J., Majeed,I.Y. and Hussein, A.O. 2018. Synthesis and spectral studies of hetrocyclic azo dye complexes with some metals. Journal of Physics.Conference Series, 1003,0120021. DOI: 10.1088/1742-6596/1003/1/012021
[27] Al-Wabli,R.I., Resmi,K., Mary,Y.S., Panicker,C.Y., Attia,M.I., El-Eman, A.A. and Alsenoy,C.V. 2016. Vibrational spectroscopic studies, fukui functions, HOMO-LUMO, NLONBO analysis and molecular docking study of (E)-1-(1,3-benzodioxol-5-yl)4,4-dimethylpent-1-en-3-one, a potential precursor to bioactive agents, Journal of Molecular Structure, 1123,375-383. DOI: 10.1016/j.molstruc.2016.07.044
[28] Hrichi,H., El-Kanzi,N.A., Ali,A.M. and Abou, A. 2023. A novel colorimetric chemosensor based on 2-[((carbamothioylhydrazazono)methyl]phenyl-4-methylbenzenesulfonate (CHMPMPS) for the detection of Cu(II) in aqueous medium, Res.Chem.Intermed., 49,2257-2276. DOI: 10.1007/s11164-022-04905-4
[29] Mohammed, I. H., Jaafar, G. H., Qaddoori, M. H., Abdulateef, M. H., & Abud, Z. T. (2021). effect of extraction on rhamnus carolnana plant in mice chromosome lymphocytes and microtubules hepg2 cancre cell line Biochemical & Cellular Archives, 21(1).

BIOGRAPHIES OF AUTHORS

<table>
<tr><td>  </td><td>**Dr. Jinan M. M. Al-Zinkee** is Associate Professor at Inorganic Chemistry Department of Chemistry, College of science, University of Diyala, Diyala, Iraq. she can be contacted at email: jinan.mohammed@uodiyala.edu.iq.</td></tr>
<tr><td>  </td><td>**Eman khalil lbrahem** is the teacher at ministry of Education she received the B.Sc degree in chemistry science from University of Diyala in lraq and M.Sc degree in chemistry science from University of Diyala . she can be contacted at email: emankhilil327@gmail.com.</td></tr>
<tr><td>  </td><td>**Dr. Amer J. Jarad is** Professor at Inorganic Chemistry Department of Chemistry, College of Education for Pure science /Ibn-Al-Haitham, University of Baghdad, Baghdad, Iraq. he can be contacted at email: **:** Amir.j.j@ihcoedu.uobaghdad.edu.iq</td></tr>
</table>